

Diversity of Methane-Cycling Archaea in Hydrothermal Sediment Investigated by General and Group-Specific PCR Primers

Mark A. Lever,^{a,b*} Andreas P. Teske^a

Department of Marine Sciences, University of North Carolina at Chapel Hill, Chapel Hill, USA^a; Center for Geomicrobiology, Department of Bioscience, Aarhus University, Aarhus, Denmark^b

The zonation of anaerobic methane-cycling *Archaea* in hydrothermal sediment of Guaymas Basin was studied by general primer pairs (*mcrI*, ME1/ME2, *mcrIRD*) targeting the alpha subunit of methyl coenzyme M reductase gene (*mcrA*) and by new group-specific *mcrA* and 16S rRNA gene primer pairs. The *mcrIRD* primer pair outperformed the other general *mcrA* primer pairs in detection sensitivity and phylogenetic coverage. Methanotrophic ANME-1 *Archaea* were the only group detected with group-specific primers only. The detection of 14 *mcrA* lineages surpasses the diversity previously found in this location. Most phylotypes have high sequence similarities to hydrogenotrophs, methylotrophs, and anaerobic methanotrophs previously detected at Guaymas Basin or at hydrothermal vents, cold seeps, and oil reservoirs worldwide. Additionally, five *mcrA* phylotypes belonging to newly defined lineages are detected. Two of these belong to deeply branching new orders, while the others are new species or genera of *Methanopyraceae* and *Methermicoccaceae*. Downcore diversity decreases from all groups detected in the upper 6 cm (~2 to 40°C, sulfate measurable to 4 cm) to only two groups below 6 cm (>40°C). Despite the presence of hyperthermophilic genera (*Methanopyrus*, *Methanocaldococcus*) in cooler surface strata, no genes were detected below 10 cm (≥60°C). While *mcrA*-based and 16S rRNA gene-based community compositions are generally congruent, the deeply branching *mcrA* cannot be assigned to specific 16S rRNA gene lineages. Our study indicates that even among well-studied metabolic groups and in previously characterized model environments, major evolutionary branches are overlooked. Detecting these groups by improved molecular biological methods is a crucial first step toward understanding their roles in nature.

Hydrothermal surface sediments in Guaymas Basin support exceptionally high microbial activity and microbial diversity (1–4). The highly productive overlying water column, combined with terrestrial runoff, leads to sedimentation rates exceeding 1 mm yr⁻¹ (5) and organic carbon contents of 2 to 4% by weight (6). In addition, the upward flow of hydrothermal fluids supplies hydrocarbons (methane, petroleum) and volatile fatty acids produced by thermal degradation of buried organic matter in deeper sediment layers to surface sediments and their microbial communities (1, 7–9).

Methanogenesis and sulfate-dependent methane oxidation in Guaymas Basin are carried out by diverse microbial lineages. 16S rRNA gene-based surveys have detected known methane-cycling groups (*Methanococcoides*, *Methanocorpusculum*, *Methanoculleus*, *Methermicoccus*, ANME-1, ANME-2) (4, 10–12), a new lineage of ANME-1, ANME-1Guaymas (12), and unknown deeply branching euryarchaeotal groups within the phylogenetic vicinity of known methane-cycling *Archaea* (4, 10). Phylogenetic analyses of *mcrA*, a gene diagnostic of methanogenic and anaerobic methanotrophic *Archaea* (13, 14), indicate an even higher diversity of methane-cycling *Archaea* than those detected by 16S rRNA gene surveys (*Methanococcoides*, *Methanohalophilus*, *Methanosaeta*, *Methanoculleus*, *Methanocorpusculum*, *Methanocaldococcus*, *Methermicoccus*, group e, ANME-1, ANME-2 [10, 12]) and, using a revised general *mcrA* primer pair (15), a novel deeply branching *mcrA* cluster (12). Perhaps surprisingly, the anaerobic methanotrophic ANME-1 cluster, a dominant group in clone libraries of archaeal 16S rRNA genes (4), was initially absent from *mcrA* clone libraries (10). This inconsistency has since been resolved by using an ANME-1-specific *mcrA* primer pair (15), with which high diversity and widespread occurrence of ANME-1 in Guaymas Basin sediment have been shown (12).

The fact that revised general and new ANME-1-specific *mcrA* primers detected a wider phylogenetic range of *mcrA* gene diversity than that obtained in previous studies on Guaymas Basin sediments (10, 11) raises several questions. (i) How do published general *mcrA* primer pairs compare in diversity coverage and detection sensitivity? (ii) To what extent do these general *mcrA* primer pairs cover the diversity of *mcrA* genes present in Guaymas Basin sediment? (iii) How do different sites within the Guaymas Basin compare in terms of methanogen and anaerobic methanotroph diversity? (iv) How do Guaymas Basin methanogenic and anaerobic methanotrophic communities compare to methanogenic and anaerobic methanotrophic communities elsewhere on Earth?

We examine these questions in surficial sediments of the Everest Mound area in the southern Guaymas vent field, home to diverse lineages of methanogens and methanotrophs (4, 10). We

Received 29 October 2014 Accepted 10 December 2014

Accepted manuscript posted online 19 December 2014

Citation Lever MA, Teske AP. 2015. Diversity of methane-cycling archaea in hydrothermal sediment investigated by general and group-specific PCR primers. *Appl Environ Microbiol* 81:1426–1441. doi:10.1128/AEM.03588-14.

Editor: C. R. Lovell

Address correspondence to Mark A. Lever, mark.lever@usys.ethz.ch.

* Present address: Mark A. Lever, Institute for Biogeochemistry and Pollutant Dynamics, Department of Environmental Systems Sciences, ETH Zürich, Zürich, Switzerland.

Supplemental material for this article may be found at <http://dx.doi.org/10.1128/AEM.03588-14>.

Copyright © 2015, American Society for Microbiology. All Rights Reserved.

doi:10.1128/AEM.03588-14

first compare the detection sensitivity and diversity coverage of three degenerate, general *mcrA* PCR primer pairs, designed by Springer et al. (13), Hales et al. (16), and more recently Lever (15). We then evaluate detection sensitivity and phylogenetic biases by comparing clone libraries based on these general *mcrA* primer pairs to ones obtained using 27 nondegenerate, group-specific *mcrA* primer pairs (15). As a further check for the phylogenetic range of general and group-specific *mcrA* primers, we compare the total community detected based on *mcrA* sequences to that detected with 17 new methanogen- and anaerobic methanotroph-targeted 16S rRNA gene primer pairs. We conclude with an analysis of methane-cycling archaeal zonation within the steep thermal and sulfate gradients of the site, investigate possible metabolic pathways of phylotypes detected based on closest relatives with known metabolisms, and compare the overall phylogenetic range and community structure to those found in previous Guaymas Basin sediment studies and other habitats worldwide.

MATERIALS AND METHODS

Sampling and site characteristics. The sediment core used in this study was obtained during Alvin Dive 3204 from the “Everest Mound” area in the southern Guaymas Trench. Temperature gradients were determined *in situ* using Alvin’s high-temperature probe. The pore water sulfate concentration profile was determined using standard ion chromatographic methods (12). An extended site description is provided in the supplemental material.

DNA extraction and primer design. DNA was extracted according to Lever et al. (17; see also the supplemental material). All primer information is shown in the supplemental material and in Table 1. The general mcrIRD primer pair and the group-specific *mcrA* primer pairs as well as all new archaeal 16S rRNA gene primers were designed based on DNA sequence alignments in the ARB software (<http://www.arb-home.de/> [18]) and tested with the DNA extracts. Annealing temperatures were based on calculated melting temperatures. For each primer pair, the lower of the two melting temperatures was used as annealing temperature.

PCR protocol. PCR assays were performed with the TaKaRa SpeedSTAR HS DNA polymerase kit (TaKaRa Bio USA, Madison, WI) using the manufacturer’s recommended reaction mixture, except that bovine serum albumin was added to a final concentration of 1 µg µl⁻¹. The PCR protocol was as follows: (i) one 2-min denaturation (98°C), (ii) 40 cycles of 10-s denaturation (98°C), 30-s annealing (Table 1 for temperatures), and 1-min extension (72°C), and (iii) one 5-min extension (72°C). For assays with general *mcrA* primers, 10 µl of DNA extract was used. For all other assays, 1 µl of extract was used. Where necessary, 1 µl of PCR product from the first PCR was transferred to tubes containing fresh PCR reagents and reamplified for a second PCR of 40 cycles.

Cloning and sequencing. PCR products were purified in a 2.5% low-melting-point agarose gel using Tris acetate-EDTA (TAE) buffer. Gel slices containing the correct PCR fragment length were excised and purified using the S.N.A.P. minikit (Invitrogen, Carlsbad, USA) and cloned into electrocompetent *Escherichia coli* using the Topo TA kit (Invitrogen, Carlsbad, CA, USA). Plasmid extraction, purification, and cycle sequencing were performed at the Josephine Bay Paul Center at the Marine Biological Laboratory (Woods Hole, MA).

Phylogenetic trees. Sequences were BLAST analyzed (www.ncbi.nlm.nih.gov/blast). Chimeras were identified by visual alignment checks in ARB and using the online software Database Enabled Code for Ideal Probe Hybridization Employing R (DECIPHER; <http://decipher.ce.wisc.edu/index.html>). Phylogenetic trees were created using ARB neighbor joining with Jukes-Cantor correction and bootstrap analyses with 1,000 replicates. The taxonomic identification and classification of novel *mcrA* phylotypes were checked and substantiated with nucleotide sequence similarity matrixes, as specified in the supplemental material.

Nucleotide sequence accession numbers. Nucleotide sequences were deposited to the GenBank archive under the following accession numbers: for *mcrA*, KM370762 to KM370786; for archaeal 16S rRNA genes, KM370787 to KM370815.

RESULTS

General results. DNA extractions were successful to 10 cm below seafloor (cmbsf), at which the sediment temperature was ~60°C (Fig. 1A). Sulfate concentrations decreased steeply in the upper cmbsf and were below the detection limit (~0.1 mM) below a 4-cm depth, indicating active sulfate reduction within the surface layers and sulfate limitation below (Fig. 1B). The absence of sulfate in the deeper sediment layers indicates minimal core disturbance and seawater in-mixing during sampling and retrieval.

The combined *mcrA* and archaeal 16S rRNA gene surveys identified a total of 22 phylotypes of methane-cycling *Archaea*. Here, distinct phylotypes were defined as having <97% sequence similarity to other sequences detected in this study; the same 97% cutoff is used consistently for *mcrA* and 16S rRNA genes. Similarly, all *mcrA* sequences from this and previous studies that shared ≥97% sequence similarity were classified as belonging to the same phylotype. A total of 21 phylotypes were detected among the *mcrA* sequences (Fig. 2), and only one additional phylotype, belonging to the candidate order “*Methanoplasmatales*,” was found among the 16S rRNA gene sequences (see Fig. S4 in the supplemental material). Several additional 16S rRNA phylotypes belonging to euryarchaeotal groups without known physiologies might, however, be involved in methane cycling. Of the phylotypes that could be linked to methane cycling based on *mcrA* detection or based on 16S rRNA gene sequences that are monophyletic with known methane-cycling *Archaea*, 20 fall into groups with known energy substrates. The remaining two *mcrA* phylotypes (termed “Deeply Branching *mcrA* groups II and III”) lack close cultured relatives or in fact any environmental sequences with high sequence similarity (Fig. 2; Table 1). The numbers of phylotypes had a bimodal distribution, with the highest numbers in cool, sulfate-containing surface samples (0 to 2 cm, ~2 to 12°C) and in a warm, sulfate-depleted layer (5 to 6 cm; ~20 to 30°C) (Fig. 2; Tables 2 and 3; see also Fig. S4 in the supplemental material). Only two phylotypes were detected below 6 cmbsf.

Among the closest BLAST hits to the 21 *mcrA* phylotypes, 8 were from Guaymas Basin sediment, 1 was from a Guaymas Basin hydrothermal vent, and 12 were from outside Guaymas Basin (Table 2). These closest BLAST hits included the pure-culture isolates *Methanocaldococcus jannaschii* and *Methanopyrus kandleri*, both of which were first isolated from a hydrothermal vent and a hydrothermal sediment in Guaymas Basin, respectively (19, 20).

***mcrA* diversity.** We designed a sequence similarity matrix for taxonomic classification of *mcrA* phylotypes that is analogous to sequence similarity cutoffs that have been employed to classify 16S rRNA gene sequences for decades (33, 34). To discuss *mcrA* diversity in consistent terms, we use the term “group” to refer to sequences classified as forming their own family, order, or class, the term “cluster” to refer to sequences classified as forming their own genus, and the term “subcluster” to refer to sequences classified as belonging to the same phylotype. In the following, we discuss *mcrA* diversity at Everest Mound based on this classification scheme. For uncultured clusters, these designations are necessarily qualified, for example, by referring to “genus level lineages.”

Within the *Methanosaecinales*, we detected 3 phylotypes in the

TABLE 1 Names, target groups, nucleotide sequences, primer lengths, amplicon lengths, annealing temperatures, and amplification success of *mcrA* and archaeal 16S rRNA gene primers with DNA extracts from Everest Mound^a

Name	Target groups	Primer sequences	No. of nucleotides	Length (bp)	T _{anneal} (°C)	Amplification ^b	Specificity ^c
<i>mcrA</i> gene primers							
<i>mcrI</i>	General	F, 5'-TAYGAYCARATHTGGYT R, 5'-ACRITCATNGCRTARTT	17;17	~490	51	+	+
ME1/ME2	General	B, 5'-CMATGCARATHGGWATGTC	20;21	~750	58	+	+
<i>mcrIRD</i>	General except ANME-1	R, 5'-CTATKGERTAGTDGERTAGT F, 5'-TWIGACCARATMGTGTY	17;17	~490	55	+	+
ANME-1- <i>mcrI</i>	ANME-1, ANME-1-related group	R, 5'-ACRITCATBKGERTARTT	20;20	~480	63	+	+
<i>mcrMS</i>	<i>Methanoscirina</i>	F, 5'-GACCACTGGTGCCTCC	20;20	425	66	+	-
mcraNME-2	ANME-2	F, 5'-TGCGCCCTGGTAGGACAGAAC	20;20	155	64	+	+
<i>mcrMsacta</i>	<i>Methanosaeta</i>	F, 5'-GGATTCAAGCAGACTACGCCAC	20;20	305	64	+	-
<i>mcrURFS</i>	Unidentified Rice Field Soil <i>McrA</i> /Zoige cluster	R, 5'-CAAGAAGCGTTGGTAGTCGA R, 5'-TATGCAACACCAAGCATACCC/GTATGCCAACAGCAGATAAC	22;21;17	385	64	+	-
mcraM-3 I	ANME-3	R, 5'-CACCGCACGTATCCTGC	20;20	525	60	-	NA
mcraM-3 II	ANME-3	F, 5'-GATIATCATAGAACAGCCG	20;22	480	64	-	NA
mcraM-3etal	ANME-3, <i>Methanomicrococcoides</i> , <i>Methanomethylovorans</i> , <i>Methanobulus</i> , <i>Methanohalophilus</i>	R, 5'-CCITGAGTGTGCACTTCCTCGT	21;17	480	60	+	-
<i>mcrFCI/FC</i>	Rice Cluster I, Fen cluster	F, 5'-AGTCAAGAGATGTCGGCCGCT	18;20	560	64	-	NA
<i>mcrFCI</i>	Fen cluster	R, 5'-CATGCTTCTTGTGCAAGGTA	19;20	510	64	-	NA
<i>mcrFCII</i>	Fen cluster	F, 5'-ACTGGTCTCTGAGTCGTCAG R, 5'-AGCCAGGTGGCATCAAGT	19;19	445	64	+	-
<i>mcrMcrop</i>	<i>Methanocorpusculum</i>	R, 5'-GACAGGTAACTGAGCGTTCA	19;20	550	64	+	-
<i>mcrMspir</i>	<i>Methanospirillum</i>	R, 5'-TCCTAGGGAAAGAACCAAG	23;20	335	56	+	-
<i>mcrMmicrob</i>	<i>Methanomicrobales</i>	F, 5'-GATGAGTACCTACTATGGTAT	21;20	310	61	+	(-/+)
<i>mcrMcul</i>	<i>Methanoculleus</i> and close relatives	R, 5'-CCTCTACTAGGTATGGACTA	23;19	290	62	+	(-/+)
<i>mcrMcuI</i>	Guaymas Basin <i>Methanomicrobales mcrA</i> cluster	R, 5'-GAGTTGGCTGAACCACACTG	21;18	355	61	+	+
<i>mcrMbacA</i>	<i>Methanobacterium aarhusense</i> group	F, 5'-GAGTTGGCTGAACCACACTG	20;22	515	63	+	-
<i>mcrMbac</i>	<i>Methanobacteriales</i> except <i>M. aarhusense</i> and <i>M. thermophilaruber</i>	R, 5'-GGTTAGGTCTTACATGTCGGT	24;23	365	63	+	(-/+)
<i>mcrMcoc</i>	<i>Methanococcaceae</i>	R, 5'-GCACACATGTCGGTAAATC/TGCTCCACACTGGTCTTG/CACCAACACTGGTCTGG	21;23	490	61	+	-/+
<i>mcrMbb</i>	<i>Methanothermobacter</i>	R, 5'-TGGTATCCGTTAGAATCTAACT	22;18	315	63	+	-
<i>mcrMpK</i>	<i>Methanopyrus kandleri</i>	F, 5'-AGCTTACACAGACAATCCIC	23;18	385	64	+	+
<i>mcrDBGrII</i>	Deeply Branching <i>mcrA</i> group II	R, 5'-CACCACACTGGCTCTGAGG	21;22	410	64	+	+
<i>mcrMlas</i>	Clone mlas, clone DEBITS and relatives	R, 5'-CTAGGATCTACATGTCGGAGG	22;18	255	64	+	-
<i>mcrDBGrIII</i>	Deeply Branching <i>mcrA</i> group III	R, 5'-GGGAGTAGTGGTACGGAGATA	18;19	395	64	+	+
<i>mcrMyrales&II</i>	<i>Methanopyrus mcrA</i> subclusters I and II	R, 5'-GTGTACAGGAGACAAACATCCGG	22;17	330	64	+	-
Archaeal 16S rRNA gene primers							
MS 18SF/MS 1138R	<i>Methanoscirina</i>	F, 5'-TGGCTGGAAATGGCTTTATGGCT R, 5'-CCGGAGGGAAATGCTGGTAA	20;19	955	65	-	-

M6 184F/MS 1009R	<i>Methanococcina</i>	F, 5'-GCTGGGATGGCTTATGGGT R, 5'-TGGCCCTACATAATTGCTGCG F, 5'-CCTAAAGATGGATCTGCGG	19; 20	825	62	+	-
MCC 231F/MCC&Mlob 1155R	<i>Methanococcoides</i> , <i>Methanolobales</i> , <i>Methanohalophilus</i>	R, 5'-CCACAGAGTACCCCATCC F, 5'-TGGTGGCGATATTGATGCTC R, 5'-TCAGGCCCTCATACAA F, 5'-TCAGGGTTAGTGGGTGTA	19; 21	934	64 ^c	+	-/+
RCI 549F/RCI 1014R	Rice Cluster 1	R, 5'-CTGACACATAGCAGCATCC F, 5'-CCTACTAGGCTACGAGCGGT R, 5'-CCCCCAATTCTTCCTTAAGTT F, 5'-TAAAGGGCTGTAGGGCC R, 5'-CCCCCAATTCTTCCTTAAGTT F, 5'-TTAACGCTATGCGACTGAGA R, 5'-TTTACGAGGGGTC F, 5'-GAGTTGCAATTAAAGCCATGTAGT R, 5'-CGACCGTACTCCCCAGAT F, 5'-GCTATCAGCCCTCGACTAACGC	22; 20	465	64 ^c	+	(-/+)
ANME-2-244F/ ANME-2-836R	ANME-2	F, 5'; 20; 20	592	60	-	NA	
Msta 268F/Msta 927R	<i>Methanosaeta</i>	R, 5'; 20; 21	659	62	+		(-/+)
Msta 571F/Msta 927R	<i>Methanosaeta</i>	F, 5'; 20; 21	356	65	+		(-/+)
MM 48F/MM 117R	<i>Methanomicrobales</i>	R, 5'; 20; 19	1123	65	+	+ +	
ANME-1-42F/ANME- 1-898R	ANME-1	R, 5'; 23; 18	856	60	+		
ANME-1 Deep 35F/ ANME-1 Deep	Deeply Branching ANME-1	R, 5'; 21; 19	1003	65	+		(-/+)
1038R		R, 5'; 21; 19	852	64 ^c	-	NA	
ANME-1 Deep 176F/ ANME-1 Deep	Deeply Branching ANME-1	R, 5'; 21; 19	852	64 ^c	-	NA	
1038R		R, 5'; 20; 19	737	62	-	NA	
MB 136F/MB 873R	<i>Methanobacteriales</i>	R, 5'; 18; 19	736	64 ^c	-	NA	
MB 137F/MB 873R	<i>Methanobacteriales</i>	R, 5'; 20; 19	563	64 ^c	-	NA	
MB 310F/MB 873R	<i>Methanobacteriales</i>	R, 5'; 19; 22	644	65	-	NA	
MC 266F/MC 910R	<i>Methanococcales</i>	R, 5'; 19; 20	786	64 ^c	+	(-/+)	
MP8MT 235F/ MT 1021R	<i>Methanopyrales</i> and <i>Methanothermatales</i>	R, 5'; 19; 20	748	64 ^c	+	(-/+)	
MP8MT 235F/ MP 983R	<i>Methanopyrales</i>	R, 5'; 19; 20	748	64 ^c	-		

^a With the exception of the mcrI and ME1/ME2 primers, which were designed by Springer et al. (13) and Hales et al. (16), all primers are from Lever (15).^b +, PCR amplification occurred; -, no PCR amplification occurred.^c +, *mcrA* genes of target group only were amplified; -/+ , *mcrA* genes of target group and others were amplified; -, only non-*mcrA* genes were amplified. NA, not applicable.

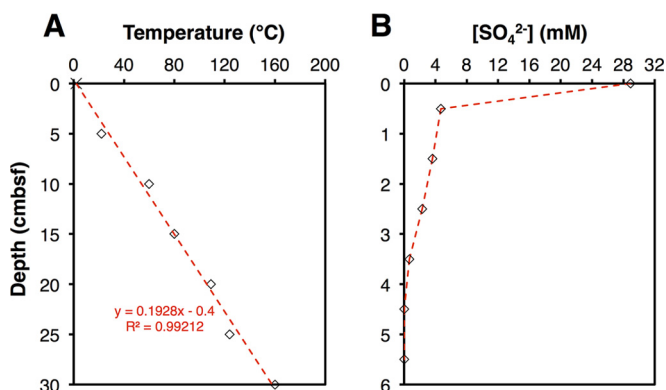


FIG 1 (A) Measured temperature data for the sediment interval examined by Weber & Jørgensen (5 to 30 cmbsf). The dashed red line indicates the best-fit line, assuming a temperature of 2°C at the sediment surface. The slope of this line was used to model temperatures at higher depth resolution throughout the sediment interval examined in this study. (B) Sulfate concentration profile. Sulfate could not be detected below 4 cmbsf.

ANME-2 family (Fig. 2), of which one is nearly identical to a previously detected sequence from Guaymas Basin. Three other phylotypes are monophyletic with *Methermicoccus shengliensis* and related environmental sequences. One of these phylotypes belongs to the same genus as *M. shengliensis*. The other two phylotypes are considerably divergent and likely belong to two additional genera within the family *Methermicoccaceae* (see Table S4 in the supplemental material). Phylotypes of *Methanohalophilus* and group e are virtually identical to previously detected sequences from Guaymas Basin sediment and a hydrothermal vent, respectively. Group e forms a sister family to the family Unidentified Rice Field Soil *mcrA* group/Zoige cluster I (represented by the sequence with accession number GU182109), which in turn forms a sister family to its neighboring branch (represented by the sequence with the accession number AY354030).

Within the *Methanomicrobiales*, a *Methanoplanus* phylotype is nearly identical to a previously detected sequence from a Guaymas Basin hydrothermal vent and closely related to *Methanoplanus petrolearius*, which was isolated from an oil field (35). Sequences of the genus level *Methanomicrobiales* seep *mcrA* cluster appear for the first time in Guaymas Basin. We also detect *mcrA* sequences of the same phylotype as a sequence previously detected in Guaymas Basin sediment (AY837767); this phylotype clusters separately from other genera of *Methanomicrobiales* and has only low DNA sequence similarity to the closest genera, *Methanoculleus* and *Methanofollis* ($83.0\% \pm 2.3\%$ and 84.1%, respectively; Fig. 2 [*Methanofollis* not shown]; see also Table S4 in the supplemental material). We classify this phylotype, which so far lacks *mcrA* sequences with high sequence similarity outside Guaymas Basin, as a member of the new genus level “Guaymas Basin *Methanomicrobiales mcrA* cluster.”

Within the *Methanococcales*, one sequence is nearly identical to *Methanocaldococcus jannaschii*; a second sequence forms a distinct phylotype with high sequence similarity to other *Methanocaldococcus* phylotypes from hydrothermal vents, including one from Guaymas Basin (Fig. 2).

Two phylotypes fall into the ANME-1 *Archaea*, which forms its own order and even a separate class along with the neighboring order level ANME-1-related group (Fig. 2; see also Table S4 in the

supplemental material). One of these phylotypes clusters with sequences from cold deep sea and mud volcano sediments. The other is nearly identical to thermophilic ANME-1 previously enriched by Holler et al. (11). All ANME-1 archaea detected here fall into the same genus level lineage. The JF937800 phylotype, which is the likely *mcrA* equivalent of the ANME-1Guaymas 16S rRNA phylotype (12), forms a separate genus level lineage together with a phylotype from hydrothermal fluid of the Endeavor Segment (HQ635748; 24). We named this lineage “Hydrothermal ANME-1 cluster.”

Within the *Methanopyrales*, we detected three different branches, all identified as members of the genus *Methanopyrus*. Besides a phylotype that is nearly identical to *Methanopyrus kandleri*, we detected a new phylotype, which we called “*Methanopyrus mcrA* subcluster I,” and one phylotype that clusters with sequences from hydrothermal vents, which we termed “*Methanopyrus mcrA* subcluster II” (Fig. 2).

In addition to the previously known groups, we detected novel deep branches on the *mcrA* phylogenetic tree, which each consist of one phylotype. We call these “Deeply Branching *mcrA* groups II and III.” Interestingly, these two groups appear equidistant to each other and to Deeply Branching *mcrA* group I: Deeply Branching *mcrA* group II has sequence similarities of 67.5 and 70.6%, and Deeply Branching *mcrA* group III has sequence similarities of 63.0 and 68.8% to the two members of Deeply Branching *mcrA* group I (see Table S4 in the supplemental material). Sequence similarities of groups II and III to each other are also low (65.7%). Based on our taxonomic classifier, Deeply Branching *mcrA* groups I, II, and III represent three distinct orders, with the two phylotypes in group I being equivalent to separate families within the same order. Our classification thus suggests that the methane-cycling *Archaea* consist of at least 10 rather than the currently recognized 7 orders (36).

Inferred energy substrates of *mcrA* phylotypes. Based on published information on the closest relatives within the *Methanomicrobiales*, *Methanococcales*, and *Methanopyrales*, which consist almost exclusively of hydrogenotrophic methanogens (19–20, 35, 37–42), H₂ and/or formate is a likely energy source of 9 of 21 *mcrA* phylotypes detected. In addition, we detected one phylotype of the genus *Methanohalophilus* and three of the family *Methermicoccaceae*, lineages that catabolize methanol and methylamines (43, 44). Aceticlastic groups (*Methanosaeta*, *Methanoscincina*, Zoige cluster I) (45–46) were not detected. ANME-1 and ANME-2 *Archaea* have been linked to anaerobic methane oxidation (47–50). Nothing is known about the substrates of group e or the two deeply branching groups.

Comparison of general *mcrA* primers. The detection sensitivity and detected number of *mcrA* clusters varied considerably between the three general primer pairs (Fig. 3). With the ME1/ME2 and mcrI primer pairs, we detected *mcrA* genes in four horizons, with only weak PCR amplification and cloning success in one of these horizons (for mcrI, 4 to 5 cmbsf; for ME1/ME2, 1 to 2 cmbsf). In contrast, the mcrIRD primer pair produced suitable PCR products for cloning throughout the upper eight horizons. The number of *mcrA* clusters was also higher; with the mcrIRD primer pair, 12 clusters were detected, compared to 10 and 7 clusters detected with the mcrI and ME1/ME2 primer pairs, respectively.

Each primer pair produced a different community profile. Not surprisingly, profiles obtained with the mcrIRD and mcrI primer

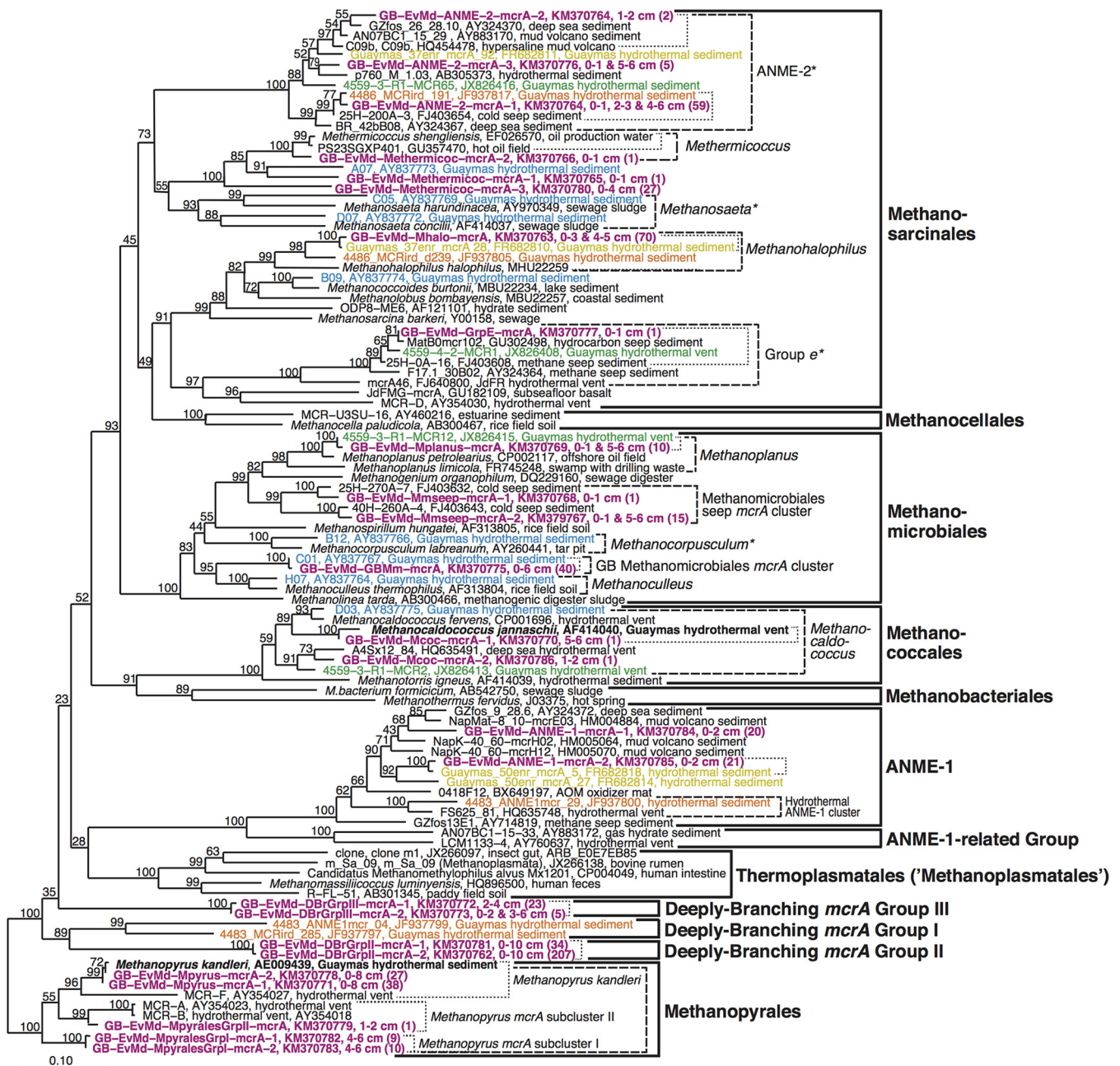


FIG 2 *mcrA* gene phylogeny. Representative phylotypes from this study are shown in bold magenta type font. The depth interval of origin is shown, along with the number of clone sequences in parentheses. Phylotypes from other studies on the Guaymas Basin have the following color codes: bold black, pure culture isolates; blue, Dhillon et al. (10); yellow, Holler et al. (11); orange, Biddle et al. (12); green, Y. He and F. Wang, unpublished data. Bootstrap values of $\geq 50\%$ are shown at branch nodes. Based on sequence similarity calculations, we made the following phylogenetic distinctions: sequences likely to belong to the same species are marked by dotted lines, dashed lines indicate members of the same genus, asterisks (*) indicate genus level *mcrA* branches that also represent families, and thick solid lines indicate sequences that belong to the same order (for more information on these calculations, see the supplemental material, as well as Discussion).

pairs, which target the same loci and are similar in primer sequence (Table 1), are more similar to one another than to the community profile obtained with the ME1/ME2 primer pair. The biggest difference is the lack of detection of group e, both deeply branching *mcrA* groups, and both *Methanopyrales* subclusters with the ME1/ME2 primer pair. Three of these five groups were detected with the *mcrI* primer pair and four with the *mcrIRD*

primer pair; mcrIRD clone libraries were even dominated by Deeply Branching group II in six of eight sediment horizons (Fig. 3).

Comparison of group-specific *mcrA* primers. Eleven of the 27 group-specific primer pairs resulted in successful *mcrA* amplifications. Five of these primer pairs exclusively amplified their target groups (Table 2; see also Table S1A in the supplemental material),

TABLE 2 Overview of phylogenotypes from within Guaymas Basin, and outside Guaymas Basin, with highest BLAST sequence similarity to ones detected at Everest Mound^a

OTU name	Closest BLAST hit from Guaymas Basin (accession no.)	Habitat	% similarity	Reference	Closest BLAST hit outside Guaymas Basin (accession no.)		Origin	% similarity	Reference(s)
					OTU name	Closest BLAST hit from Guaymas Basin (accession no.)			
<i>mcrA</i> genes									
GB-EvMd-Mhalo-mcrA	<i>Guaymas_37enr_mcrA_28</i> (FR#82810)	Hydrothermal sediment	99	11	<i>Methanotadphilus halophilus</i> (AB703633)	Shark Bay hypersaline microbial mat	86	21	
GB-EvMd-GrpE-mcrA	4559-4-2-MCR1 (JX826408)	Hydrothermal vent	98	Y. He and F. Wang, unpublished	25H_0A_16 (FJ403608)	Sea of Okhotsk cold seeps	99	22	
GB-EvMd-ANME-2-mcrA-2	4559-3-R1-MCR65 (JX826416)	Hydrothermal vent	93	Y. He and F. Wang, unpublished	C09b (HQ454478)	Napoli mud volcano	97	23	
GB-EvMd-ANME-2-mcrA-1	4486_MCRird_191 (FJ937817)	Hydrothermal sediment	99	12	25H_200A_3 (FJ403654)	Sea of Okhotsk cold seeps	99	Zhang et al., unpublished	
GB-EvMd-ANME-2-mcrA-3	<i>Guaymas_37enr_mcrA_92</i> (FR#82811)	Hydrothermal sediment	93	11	p760_M_1_03 (AB305373)	Okinawa Trough hydrothermal sediment	95	24	
GB-EvMd-Methermicoc-mcrA-2	A07 (AY837773)	Hydrothermal sediment	82	10	PS23SGXP401 (GU357470)	Hot Alaskan oil field	96	25	
GB-EvMd-Methermicoc-mcrA-1	A07 (AY837773)	Hydrothermal sediment	85	10	FS448_53 (HQ635543)	Mariana Arc, hydrothermal vent fluid	94	26, 27	
GB-EvMd-Methermicoc-mcrA-3	A07 (AY837773)	Hydrothermal sediment	77	10	PS23SGXP401 (GU357470)	Hot Alaskan oil field	83	25	
GB-EvMd-Mnseep-mcrA-2	4559-3-R1-MCR12 (JX826415)	Hydrothermal vent	82	Y. He and F. Wang, unpublished	40H_260A_4 (FJ403643)	Sea of Okhotsk cold seep	98	Zhang et al., unpublished	
GB-EvMd-Mnseep-mcrA-1	None				25H_270A_7 (FJ403632)	Sea of Okhotsk cold seep	96	Zhang et al., unpublished	
GB-EvMd-Mplanus-mcrA	4559-3-R1-MCR12 (JX826415)	Hydrothermal vent	99	Y. He and F. Wang, unpublished	LW-6 (JX430031)	Min River estuary	92	C.-X. She and C. Tong, unpublished	
GB-EvMd-Mcull-mcrA	C01 (AY3767)	Hydrothermal sediment	99	10	ATB-EN-10393-M138 (FJ226731)	Agricultural biogas plant	87	28	
GB-EvMd-Mcoc-mcrA-1	<i>Methanocaldibacillus jannaschii</i> (L77117)	Hydrothermal sediment	99	19	FS25_56 (HQ635721)	Juan de Fuca Ridge hydrothermal vent fluid	99	26	
GB-EvMd-Mcoc-mcrA-2	4559-3-R1-MCR2 (JX826413)	Hydrothermal sediment	96	Y. He and F. Wang, unpublished	A4Sx12_84 (HQ635491)	Juan de Fuca Ridge hydrothermal vent fluid	95	26	
GB-EvMd-ANME-1-mcrA-1	None				NapMat-8_10-mcrE03 (HM004884)	Napoli mud volcano	92	23	
GB-EvMd-ANME-1-mcrA-2	<i>Guaymas_50enr_mcrA_63</i> (FR#82818)	Hydrothermal sediment	98	11	NapK-40_-60-mcrH12 (HM005070)	hypersaline sediment	92	29	
GB-EvMd-DbrGrpII-mcrA-1	4483_MCRird_285 (JF937797)	Hydrothermal sediment	72	12	M_mcrA-11 (JQ406852)	Huabei oil field	72	30	
GB-EvMd-DbrGrpII-mcrA-2	4483_MCRird_285 (JF937797)	Hydrothermal sediment	71	12	M_mcrA-11 (JQ406852)	production water	72	30	
GB-EvMd-DbrGrpIII-mcrA-1	<i>Methanopyrus kandleri</i>	Hydrothermal sediment	71	20	FS625_63 (HQ635729)	Juan de Fuca Ridge hydrothermal vent fluid	74	26	
GB-EvMd-DbrGrpIII-mcrA-2	<i>Methanopyrus kandleri</i>	Hydrothermal sediment	71	20	FS625_63 (HQ635729)	Juan de Fuca Ridge hydrothermal vent fluid	75	26	
GB-EvMd-MpyralsGrpI-mcrA	<i>Methanopyrus kandleri</i>	Hydrothermal sediment	88	20	MCR-A (AY354023)	EPR diffuse vent covered by mats	94	31	
GB-EvMd-MpyralsGrpII-mcrA-1	<i>Methanopyrus kandleri</i>	Hydrothermal sediment	86	20	MCR-B (AY354018)	EPR diffuse vent covered by mats	89	31	
GB-EvMd-MpyralsGrpII-mcrA-2	<i>Methanopyrus kandleri</i>	Hydrothermal sediment	86	20	MCR-B (AY354018)	EPR diffuse vent covered by mats	89	31	
GB-EvMd-Mpyrus-mcrA-2	<i>Methanopyrus kandleri</i>	Hydrothermal sediment	99	20	1crD2T36 (FN650318)	Rainbow ultramafic hydrothermal vent fluid	89	32	
GB-EvMd-Mpyrus-mcrA-1	<i>Methanopyrus kandleri</i>	Hydrothermal sediment	99	20	1crD2T36 (FN650318)	Rainbow ultramafic hydrothermal vent fluid	90	32	

Archaeal 16S rRNA genes GB-EvMd-Methemicroc-A	4A08 (AY835419)	Hydrothermal sediment	97	10	<i>Methermicoccus shengliensis</i> (NR_043960) <i>Methermicoccus shengliensis</i> (NR_043960)	Shengli oil field, production water	99	44
GB-EvMd-Methemicroc-C	4A08 (AY835419)	Hydrothermal sediment	100	10	SS_WC_06 (FJ656258)	Shengli oil field, production water	99	44
GB-EvMd-Halo-C	GUAY_3'env_Arch72 (FR682485)	Hydrothermal sediment	99	51	QHYA-25 (JF741950)	Salton Sea, hypersaline lake sediment	99	56, 57
GB-EvMd-Mcull-A	7H12 (AY835412)	Hydrothermal sediment	99	10	<i>Methanoculleus</i> sp. clone A3 (AJ133793)	Oil reservoir	96	Tang et al., unpublished
GB-EvMd-Mcull-B	7H12 (AY835412)	Hydrothermal sediment	100	10		Freshwater sediment enriched with hexadecane	96	58
GB-EvMd-MBGD-A	4559-4-C2-82 (JX507259)	Hydrothermal vent	98	Y. He and F. Wang, unpublished	KSTWh-Cl-7-A-028 (JQ611039)	Kueishan is shallow hydrothermal field	90	Lin et al., unpublished
GB-EvMd-MBGD-B	4559-4-C2-82 (JX507259)	Hydrothermal vent	98	Y. He and F. Wang, unpublished	IAN1-62 (AB175394)	Okinawa Trough, hydrothermal vent chimney	92	59
GB-EvMd-Mplastnatales	7C08 (AY835423)	Hydrothermal sediment	99	10	0DA-79 (JQ772440)	High-temperature oil reservoir	99	Z. Fang, unpublished
GB-EvMd-DHVE5-A	None			a87R29 (DD417481)	EPR, seafloor basaltic flanks	97	60	
GB-EvMd-DHVE5-B	None			ARCHDER07_1A1 (FN598017)	Almeria, Spain, seawater- processed activated sludge	88	61	
GB-EvMd-ANME-1a-B	GUAY_50env_Arch41 (FR682490)	Hydrothermal sediment	99	11	MCH18_26C2 (HM600925)	Gulf of Mexico hydrocarbon seep	99	Twing et al., unpublished
GB-EvMd-ANME-1a-C	Arch4483_112 (JF937751)	Hydrothermal sediment	99	12	MCH18_26C2 (HM600925)	Gulf of Mexico hydrocarbon seep	99	Twing et al., unpublished
GB-EvMd-ANME-1b-A	BG410(1)9 (JQ740749)	Hydrothermal vent fluid	99	27	FS725(3)73 (JQ740760)	Endeavor Segment hydrothermal fluid	97	27
GB-EvMd-ANME-1b-C	GBa2r032 (AF419632)	Hydrothermal sediment	99	4	FS625(3)16 (JQ740759)	Endeavor Segment hydrothermal fluid	99	27
GB-EvMd-GBEury-G	Arch4486_075 (JF937738)	Hydrothermal sediment	99	12	KZNMV-25-A37 (JF712390)	Kazan Mud Volcano, hydrate sediment	100	62
GB-EvMd-GBEury-E	Arch4486_075 (JF937738) 4E09 (AY835427)	Hydrothermal sediment	96	12	Arch-O12 (JQ241421)	Huabei oil field	98	63
GB-EvMd-GBEury-K	Thermococcus sp. GB18 (JF862790)	Hydrothermal sediment	98	10	KZNMV-25-A37 (JF712390)	Kazan Mud Volcano, hydrate sediment	95	62
GB-EvMd-ThCoc-D	<i>Thermococcus</i> sp. GB18 (JF862790)	Hydrothermal sediment	99	52	<i>Thermococcus alcaliphilus</i> (NR040870)	Vulcano submarine solfataric field	99	64
GB-EvMd-ThCoc-E	<i>T. mexicanus</i> (AY099181) (JQ346762)	Hydrothermal sediment	99	53	HibPWCL-ARC3 (JF789485)	Hibernia oil field, production water	99	Yeung et al., unpublished
GB-EvMd-ThCoc-F		Sulfide chimney	95	K. Longnecker and A.-L. Reysenbach, unpublished	Thermococcus sp. Ax00-27 (AY559130)	Axial seamount, diffuse hydrothermal vent	97	J.A. Huber and J.A. Baross, unpublished
GB-EvMd-ThCoc-G	G26_C48 (AF356631)	Sulfide chimney	95	K. Longnecker and A.-L. Reysenbach, unpublished	Q2-a15.seq (FR852947)	Hydrothermal vent chimney	94	J. Li, unpublished
GB-EvMd-Archaeglobales	<i>Archaeoglobus profundus</i> (AF297529)	Hydrothermal sediment	93	54	PW15.7A (EU573156)	North Sea chalk petroleum reservoir	98	65
GB-EvMd-DHVEG	90-PY-10 (FR692155)	Hydrothermal sediment	99	55	pCIRAL (AB095122)	Central Indian Ridge hydrothermal field	96	66
GB-EvMd-AcidProf-A	G26_C56 (AF356635)	Sulfide chimney	98	K. Longnecker and A.-L. Reysenbach, unpublished	HTM1039Pn-A31 (AB611429)	Okinawa Trough, polychaete nest, hydro. vent	99	67
GB-EvMd-AcidProf-B	G26_C56 (AF356635)	Sulfide chimney	98	K. Longnecker and A.-L. Reysenbach, unpublished	<i>Acidiliprofundum</i> isolate EPR07-39 (FR865186)	EPR hydrothermal vent	99	68

(Continued on following page)

TABLE 2 (Continued)

OTU name	Closest BLAST hit from Guaymas Basin (accession no.)	Habitat	% similarity	Reference	Closest BLAST hit outside Guaymas Basin (accession no.)	Origin	% similarity	Reference(s)
GB-EvMd-AcidProfFF	G26_C56 (AF356635)	Sulfide chimney	95	K. Longnecker and A.-L. Reysebach, unpublished	<i>Acidifiprofundum</i> isolate EPR07-39 (FR865186)	EPR hydrothermal vent	96	68
GB-EvMd-MCG-A	4559-4-C2-11 (JX507250)	Hydrothermal vent	99	Y. He and F. Wang, unpublished	PNG_Kap4_A49 (JF935159)	Alkaline hot spring	99	Amend et al., unpublished
GB-EvMd-MCG-B	4559-4-C2-9-5 (JX507244)	Hydrothermal vent	97	Y. He and F. Wang, unpublished	A257-49 (FN554070)	Logatchev ultramafic hydrothermal vent field	98	69
GB-EvMd-Thermoproteales-1	4559-4-C2-61 (JX507245)	Hydrothermal vent	100	Y. He and F. Wang, unpublished	HTM1036Pn-A14 (AB611436)	Okinawa Trough, polychaete nest, hydrothermal vent	96	67

^aBoldface indicates the environmental sequences with the highest sequence similarity to the operational taxonomic units (OTU) detected in this study. Unpublished data: Amend et al., J. P. Amend, L. C. Burcea, and D. R. Meyer-Dombard; Lin et al., L.-H. Lin, W.-X. Tu, W.-Y. Tsai, and T.-W. Cheng; Tang et al., Y.-Q. Tang, Y. Guang, Y. Li, M. Cai, and X.-L. Wu; Twing et al., K. Twing, J. Biddle, C. Martin, K. Lloyd, and A. Teske; Yeung et al., W. C. Yeung, K. Lee, S. Cobanli, T. King, J. Bugden, L. G. Whyte, and C. W. Greer; Zhang et al., L. Zhang, H. Dang, and X. Luan.

which are ANME-1 *Archaea*, ANME-2 *Archaea*, *Methanopyrus kandleri*, and Deeply Branching *mcrA* groups II and III.

In contrast to our results with the general *mcrA* primers, we detected only one new phylotype (ANME-1) using group-specific primers (Table 3). Moreover, certain phylotypes were detected in depth intervals, where they had not been detected with general primer pairs, e.g., *Methanopyrus kandleri* at 1 to 2 cm, ANME-2 at 2 to 3 cm, and most strikingly, Deeply Branching group III, which was shown to be present from 0 to 6 cmbsf rather than only from 2 to 3 cmbsf. Interestingly, with the notable exception of ANME-1, primer pairs that were designed to target previously undetected groups, e.g., *mcrMsae* for *Methanosaeta* or *mcrMbac* for *Methanobacteriales*, still did not detect these groups. Instead, they amplified nontarget *mcrA* clusters already detected with general primers (*mcrMbac*) (Table 3) or non-*mcrA* genes (*mcrMsae*) (Table 1A). Moreover, certain clusters detected with general primers, e.g., *Methanoplanus*, *Methanocaldococcus*, or *Methanopyrus mcrA* subclusters I and II were not detected with group-specific primers. These primers amplified (i) not all their target groups (*McrMm* in the case of *Methanoplanus*), (ii) nontarget *mcrA* (*Methanocaldococcus*), or (iii) non-*mcrA* genes (*Methanopyrus mcrA* subclusters I and II) (Table 2; see also Table S1A in the supplemental material).

Archaeal 16S rRNA gene diversity. The archaeal 16S rRNA gene survey yielded a total of 14 lineages and 29 phylotypes (Table 2; see also Fig. S4 in the supplemental material). Five euryarchaeotal lineages belong to known methane-cycling groups: the methyl-disproportionating genera *Methanohalophilus* and *Methermicoccus* within the *Methanosarcinales*, the methylotrophic order *Methanoplasmatales*, the members of which gain energy by methanol reduction with H₂ (71, 72), and the likely hydrogenotrophic sister lineage of *Methanoculleus* within the hydrogenotrophic *Methanomicrobiales* (the plausible 16S rRNA gene equivalent of the Guaymas Basin *Methanomicrobiales mcrA* cluster), as well as the ANME-1 methane oxidizers. Phylotypes from four groups with cultured members—the *Thermococcales*, *Archaeoglobales*, *Thermoproteales*, and the Deep-Sea Hydrothermal Vent Euryarchaeotal group 2 (DHVE2) (73)—are not linked to methane cycling. The remaining phylotypes are from uncultured lineages: the Guaymas Euryarchaeotal group (10), the Marine Benthic group D (74), the Deep-Sea Hydrothermal Vent Euryarchaeotal group 5 (DHVE5) (73), the Deep-Sea Hydrothermal Vent Euryarchaeotal group/Rice Cluster V (DHVEG/RC-V) (66, 75), and the Miscellaneous Crenarchaeotal group (MCG) (76, 77). Though primer pairs were designed to target groups of *Euryarchaeota*, they also amplified phylotypes of crenarchaeotal MCG and *Thermoproteales*. The archaeal 16S rRNA gene lineages are further discussed in the supplemental material.

All 16S rRNA gene lineages were previously detected in sediments or hydrothermal vents of the Guaymas Basin, with the exception of the DHVE5 (Table 2; see also Fig. S4 in the supplemental material). Of the phylotypes detected, approximately one-half (14) had the closest BLAST hits from within the Guaymas Basin, including hydrothermal vents and hydrothermal sediments in roughly equal proportions. The other phylotypes (15) had the closest BLAST hits from outside the Guaymas Basin, mainly from hydrothermal vents, oil reservoirs, cold seeps, and mud volcanoes.

DISCUSSION

Methane cycling archaeal lineages. Our study demonstrates a diversity hot spot for methane-cycling archaea in Guaymas Basin sediments. Collectively, the *mcrA* and 16S rRNA gene data include at least 22 phylotypes, of which 21 were among sequenced *mcrA* genes. The only known methane-cycling archaea detected with 16S rRNA gene primers but missed with the *mcrA*-targeted approach were the *Methanoplasmatales* (Fig. 2; see also Fig. S4 in the supplemental material).

The *mcrA* diversity exceeds the cumulative diversity detected in previous *mcrA* gene surveys in Guaymas sediments (10, 12; see Table 5). As did previous studies, we detected phylotypes of the methylotrophic *Methanosarcinales*, hydrogenotrophic *Methanomicrobiales* and *Methanococcales*, and anaerobic methanotrophic ANME-1 and ANME-2 Archaea. Seven of these share the same phylotype ($\geq 97\%$ sequence similarity) with *mcrA* sequences that were previously detected in Guaymas Basin (Fig. 2). The key differences from past studies are the detection of two novel deeply branching *mcrA* clusters and the first detection of *Methanopyrus* in a genetic survey of sediment. Our sequence similarity analyses also suggest two new genus level lineages in the family *Methermicoccaceae*, one of which was previously detected but not phylogenetically assigned (AY837773) (10), as well as the presence of the genus *Methermicoccus*.

We confirm that previous failures to detect ANME-1 Archaea using general *mcrA* primers are due to primer bias of general *mcrA* primers against this group (12, 15). This problem is overcome by running PCR assays with ANME-1-specific *mcrA* primers complementarily to ones with general *mcrA* primers.

Inferred energy substrates. (i) Hydrogenotrophic methanogens. Five of the *mcrA* branches detected have high sequence similarity to cultivated, obligate H₂- and formate-utilizing methanogens (Fig. 2; Table 4); thus, H₂ and/or formate are likely to be important *in situ* methanogenic substrates. This finding implies that microbial sulfate reduction in the upper centimeters (0 to 4 cmbsf; Fig. 1B), is not drawing H₂ concentrations below the threshold required by methanogens, unlike in coastal sediments (78). Fluctuating redox conditions, caused by temporal shifts in advection of highly reduced hydrothermal fluids and oxygenated bottom seawater through surficial sediment (79), may prevent anaerobic microbes from exerting a thermodynamic control over H₂ concentrations. Interestingly, while two clusters were detected throughout (Guaymas Basin *Methanomicrobiales mcrA* cluster, *Methanopyrus*), the three remaining clusters were detected only in surface sediments (0 to 2 cmbsf) and in one deeper layer (5 to 6 cmbsf; *Methanomicrobiales mcrA* seep cluster, *Methanoplanus*, *Methanocaldococcus*) (Table 4). This bimodal distribution may reflect local peaks in hydrogenotrophic activity and different H₂ sources, for example microbial diagenesis near the surface and thermal degradation of organic matter in deeper layers.

(ii) Methylotrophic methanogens. The detection of *mcrA* and 16S rRNA genes with high sequence similarity to known methylotrophic methanogens (Fig. 2; see also Fig. S4 in the supplemental material) is consistent with past studies on Guaymas Basin sediments (Table 5) (10, 12). These phylotypes were detected throughout the upper 5 cm across a range of temperatures (2 to 33°C) and sulfate concentrations (0 to 4 mM). Yet, if clone libraries obtained with general *mcrA* primers are an indication (Fig. 3), the proportion of methylotrophs of the total methane-cycling

TABLE 3 Depth intervals in which various *mcrA* clusters were detected using general and group-specific primers^a

Primer	Depth (cmbsf)		No. of <i>mcrA</i> clusters (of 14)									
	GB	DB	<i>Methanopyrus</i>	<i>Methanopyrus</i>	<i>Methanopyrus</i>	<i>Methanopyrus</i>	<i>Methanopyrus</i>	<i>Methanopyrus</i>	<i>Methanopyrus</i>	<i>Methanopyrus</i>	<i>Methanopyrus</i>	<i>Methanopyrus</i>
ME1/MEE2	0–1, 5–6	0–1, 5–6	0–1, 4–5	0–2, 4–5	0–1	0–1, 2–3	0–1, 2–3	0–1, 2–3	0–1, 2–3	0–1, 2–3	0–1, 2–3	0–1, 2–3
<i>mcrI</i>	0–1	0–1	0–1, 2–3, 4–5	5–6	2–3, 4–6	0–1	0–1, 2–3	0–1, 2–3	0–1, 2–3	0–1, 2–3	0–1, 2–3	0–1, 2–3
<i>mcrIRD</i>	0–1	0–1, 5–6	0–3	1–2	0–1, 2–8	0–3	0–4	0–1	0–1	0–1	0–1	0–1
<i>mcrANME-1</i>								0–2	0–1	0–1	0–1	0–1
<i>mcrANME-2</i>								0–2	0–1	0–1	0–1	0–1
<i>mcrFCI</i>								0–2	0–10	0–10	0–10	0–10
<i>mcrMicrom</i>								0–2	0–1	0–1	0–1	0–1
<i>mcrMacI</i>								0–3	0–3	0–3	0–3	0–3
<i>mcrMac</i>								0–3	0–3	0–3	0–3	0–3
<i>mcrMacC</i>								0–8	0–2	0–1	0–1	0–1
<i>mcrMpK</i>								2–3	2–3	2–3	2–3	2–3
<i>mcrDGrII</i>								0–10	1–2, 3–4	2–4	2–4	2–4
<i>mcrDGrIII</i>								0–6	0–6	1	1	1

^a Only data for group-specific primer pairs that successfully amplified *mcrA* genes are shown.

^b To simplify, all three *Methermicoccaceae* genus level phylotypes treated as one cluster in this table.

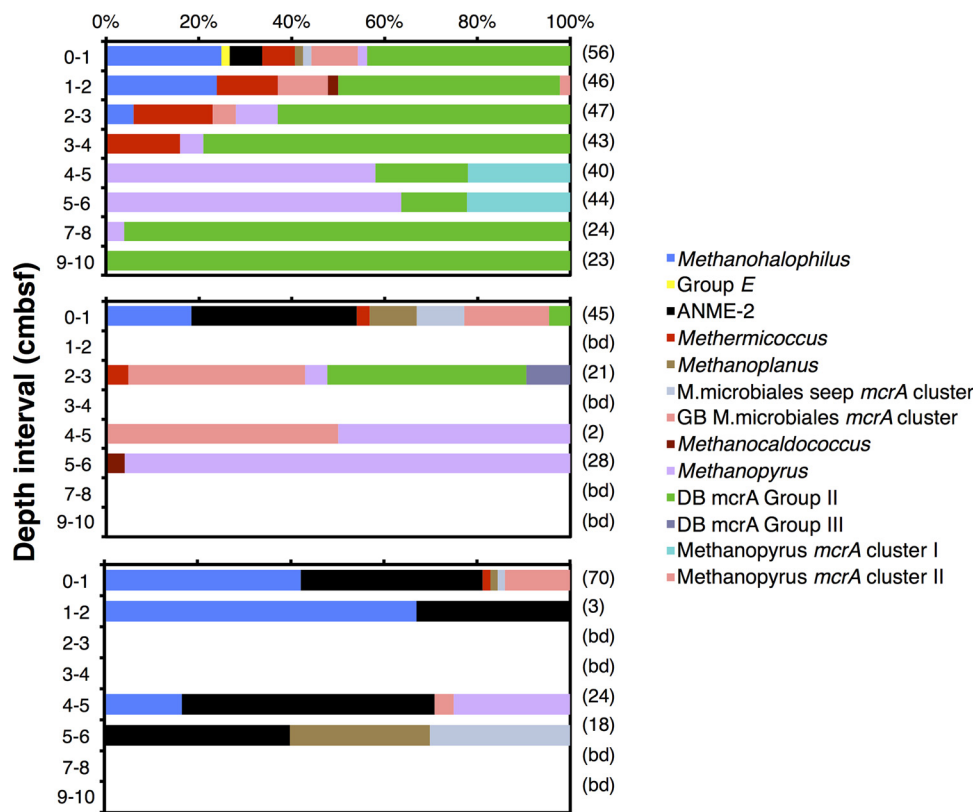


FIG 3 Comparison of primer performance versus depth using the three general *mcrA* primer pairs. (Top panel) mcrIRD primer pair; (middle panel) mcrI primer pair; (bottom panel) ME1/ME2 primer pair. After these initial clone libraries, which led to the use of the mcrIRD primer pair from then on, additional sequencing on new PCR products was done with the mcrIRD primer pair, resulting in detection of further clusters (Table 3). We omit these results here to make primer performances more comparable.

community decreases downward. In line with this interpretation, methylotrophy at our site is probably supported mainly by the biological production of methylamines and/or methanol from photosynthesis-derived organic matter.

(iii) Anaerobic methanotrophs. The presence of *mcrA* genes of ANME-1 and ANME-2 *Archaea* suggests that anaerobic methanotrophy (AOM) is concurrent with methanogenesis. If anaerobic methanotrophy is a reversal of methanogenesis (80) and coupled to sulfate reduction via syntrophic activity by sulfate-reducing bacteria (49), then the coexistence of methanogenesis and methanotrophy in the same samples is thermodynamically possible under two scenarios: the presence of chemically distinct microenvironments or pulsating hydrothermal and bottom seawater flow resulting in redox conditions that are alternatingly favorable for methanogenesis and AOM. While the existence of microniches has not been determined, there is evidence in support of the latter scenario (79, 81). Alternatively, anaerobic methanotrophy may not be a reversal of methanogenesis and thus readily cooccur with methanogenesis. Recent studies on ANME-2 *Archaea* suggest that these methanotrophs can intracellularly couple the oxidation of methane to the reduction of elemental S⁰ (50).

(iv) Acetoclastic methanogens. The absence of identifiable acetoclastic methanogens in this survey may seem puzzling, given that acetate is a key intermediate in the anaerobic microbial breakdown of organic matter (82) and produced by thermal degradation or organic matter (83). Acetate is also known to occur at

locally high pore water concentrations in Guaymas Basin sediments (8, 10), and *mcrA* sequences of the acetoclastic genus *Methanosaeta* were previously detected in Guaymas Basin sediments (10), and in oil- and hydrocarbon-rich environments elsewhere (62, 84–86). Plausible explanations are as follows: (i) *mcrA* phylotypes detected are unrecognized acetoclastic methanogens; the primary suspects are the uncultivated group e and Deeply Branching *mcrA* groups II and III, and especially group e, which belongs to the *Methanosarcinales*, an order that includes the acetoclastic *Methanosarcina*, Unidentified Rice Field Soil *McrA/Zoige* cluster I (represented by the sequence with accession number GU182109), and *Methanosaeta*; (ii) acetate is consumed by other metabolic guilds; the genetic potential for acetate oxidation is present based on 16S rRNA gene sequences of archaeal groups that oxidize acetate with sulfate, S(0), Fe(III), nitrate, or nitrite as electron acceptors (see the supplemental material); and (iii) failure of our PCR primers to detect acetoclastic methanogens. The last scenario is the least likely, given that the mcrIRD primer pair PCR amplifies all three known groups of acetoclastic methanogens in samples from other locations (15, 17; M. A. Lever, unpublished data) and that group-specific primers also did not result in their detection (Table 1).

(v) The unknowns. The energy substrates used by the five uncultivated lineages are unknown, and phylogenetic affiliation can suggest only working hypotheses. The two phylotypes clustering with the methanol-disproportionating *Methermicoccus shenglien-*

TABLE 4 Substrate use by closest relatives of all 14 *mcrA* clusters, depth intervals and temperature ranges in which they were detected, and total number of *mcrA* clusters detected per depth layer^a

Depth (cmbsf)	Temp (°C)	<i>Methanoplatus</i> ^f	<i>Methanomicrobates</i>	<i>Methanomicrobales</i>	<i>H₂/HCO₃</i> , formate		MeOH, TMA	Methane	Unknown ^b	No. of clusters (of 12) per depth layer	
					<i>mcrA</i> seep cluster	<i>mcrA</i> cluster					
0–1	2–7	+								11	
1–2	8–12	+								11	
2–3	13–17	–	–							7	
3–4	18–23	–	–							5	
4–5	24–28	–	–							7	
5–6	29–33	–	–	–	–	–	–	–	–	10	
7–8	39–43	–	–	–	–	–	–	–	–	2	
9–10	49–54	–	–	–	–	–	–	–	–	1	
12–13	64–69	–	–	–	–	–	–	–	–	0	
15–16	85–89	–	–	–	–	–	–	–	–	0	
19–20	100–105	–	–	–	–	–	–	–	–	0	
No. of depth intervals	NA	3	3	6	2	7	4	4	2	5	1
										8	8
										6	6
										NA	NA

^a Includes data obtained with all primers used in this study. Abbreviations and symbols: MeOH, methanol; TMA, trimethylamine; +, detected; –, not detected; NA, not applicable.

^b Unknown, groups with no cultured relatives.

^c In pure culture.

^d Includes *Methanopyrus mcrA* subclusters I and II.

^e All three *Methermicoccaceae* genus-level phylogenotypes are treated as one cluster in this table.

^f Not in pure culture; evidence from radiotracer studies.

sis belong to the same family, the *Methermicoccaceae*, and could equally represent methylotrophic methanogens. Group e is a candidate for generalistic methanogens, due to its clustering with the Unidentified Rice Field Soil *mcrA*/Zoige cluster I group, members of which use H₂, acetate, methanol, and methylamines as energy substrates (46). Such inferences are impossible for Deeply Branching *mcrA* groups II and III. The *mcrA* sequence similarity of both groups to the closest cultured relative, *Methanopyrus kandleri*, is low (~67%) (see Table S4 in the supplemental material), so low that our taxonomic classifier indicates Deeply Branching *mcrA* groups II and III to belong to a different order or even class from *Methanopyrus kandleri* (see Fig. S3 in the supplemental material).

Biogeographical implications. The high DNA sequence similarity of many phylotypes detected in this study to ones detected at other Guaymas Basin sites as well as in hydrothermal environments, oil reservoirs, and hydrocarbon seeps worldwide is striking—as is the near absence of highly similar DNA sequences from other well-studied methanogenic environments, such as sewage digesters, bovine intestines, rice fields, freshwater, and estuarine and marine sediments (Table 2; see also Table S5 in the supplemental material). This indicates that the global distribution of methane-cycling *Archaea* follows biogeographic patterns. Methane-cycling *Archaea* may populate Guaymas Basin sediments in exceptional phylogenetic diversity because these sediments combine key characteristics of hydrothermal environments, oil reservoirs, and hydrocarbon seeps. These characteristics are as follows: (i) hydrothermal fluid flow and circulation, which produce a dynamic environment with profound physicochemical changes over short distances and time scales, (ii) abundance of petroleum compounds and hydrocarbons produced thermogenically from relict organic carbon, and (iii) high supply of microbial energy substrates by thermal degradation of relict organic carbon, petroleum compounds, and hydrocarbons and by microbial fermentation of photosynthesis-derived organic matter, petroleum compounds, and hydrocarbons. Thus, the exceptional diversity of methane-cycling *Archaea* in sediments of the Guaymas Basin could reflect the fact that these sediments host the cumulative diversity of ecological niches that are otherwise found in three physically separated habitat types.

In addition to high diversity, the discovery of three deeply branching groups, each likely to represent a new order of methane-cycling *Archaea*, raises the questions as to why these groups were first detected here and which characteristics of Guaymas Basin sediment select for their presence. Surface sediments of Guaymas Basin are a distinctive environment because they combine extreme fluctuations in temperature, fluid flow, and redox conditions with exceedingly high energy fluxes. We propose that high energy availability combined with high physiological stress and mortality due to frequent physicochemical disturbances prevents the establishment of microbial climax communities and enables disturbance-resilient groups that are competitively excluded in more stable environments to thrive here.

Primer recommendation. Our study underscores the importance of using suitable general and lineage-specific PCR primers to detect and accurately map the phylogenetic diversity of (unknown) microorganisms. Comparisons of primer performance and phylogenetic coverage (discussed in detail in the supplemental material) suggest that the mcrIRD primer pair, when combined with the ANME-1-*mcrA* primer pair, covers a wide diversity of *mcrA* genes. Though we cannot preclude that certain divergent

TABLE 5 Comparison of *mcrA* community profiles across three environmental surveys in the Guaymas Basin

Characteristic (unit)	Everest Mound, Alvin dive 3205 (Dhillon et al. [10])	Biddle et al. (12)	Megamat, Alvin Dive 4486	UNC Mat, Alvin Dive 4489	Everest Mound, Alvin dive 3204 (this study)
Location	Lat 27.0148, long -111.4122	Lat 27.0065, long -111.4093	Lat 27.0077, long -111.4085	Lat 27.0074, long -111.4088	Lat 27.0149, long -111.4105
Sediment depth (cmbsf)	0–15	8–10	6–8	8–14	0–10
Temp (°C)	3–94	15–20	30–35	60–95	~2–54
Sulfate concn (mM)	0–19	~8–25	~24–28	~22–29	0–4
Other descriptors	No mat, hydrocarbon rich	White and orange <i>Beggiatoa</i> mat	Edge of white <i>Beggiatoa</i> mat, hydrocarbon rich	Orange <i>Beggiatoa</i> mat	Patchy mat, hydrocarbon rich
<i>mcrA</i> phylotypes detected					
Methylotrophic					
<i>Methanococcoides</i>	+		+		
<i>Methanohalophilus</i>			+		+
<i>Methermicoccaceae</i>	+				+
Aceticlastic					
<i>Methanosaeta</i>	+				
Hydrogenotrophic					
<i>Methanoplanus</i>					+
GB <i>Methanomicrobiales</i> <i>mcrA</i> cluster	+				+
<i>Methanomicrobiales</i>					+
Seep <i>mcrA</i> cluster					
<i>Methanocorpusculum</i>	+	+			
<i>Methanocaldococcus</i>	+				+
<i>Methanopyrus</i>					+
Methanotrophic					
ANME-1		+	+		+
ANME-2	+		+		+
Unknown					
Group e			+		+
Deeply Branching <i>mcrA</i> group I		+			
Deeply Branching <i>mcrA</i> group II					+
Deeply Branching <i>mcrA</i> group III					+

sequences are missed, our results show that the mcrIRD primers perform well beyond the range of known *mcrA* sequences and even amplify novel, deeply branching groups. The mcrIRD primer pair thus combines wide phylogenetic breadth with a lower detection limit than the mcrI and ME1/ME2 primer pairs and illustrates how reduced primer degeneracy and hence higher amplification efficiency do not necessarily compromise the breadth of phylotypes targeted. The new phylotypes and *mcrA* gene lineages detected show that the methanogenic and methane-oxidizing archaea—a metabolic guild generally thought of as well explored—are considerably more diverse than expected and contain previously uncharacterized “microbial dark matter” (87) that needs genomic and physiological investigation.

ACKNOWLEDGMENTS

Sediment sampling in Guaymas Basin in 1998 was made possible by NSF grant OCE 9714195 (Life in Extreme Environments) to A.P.T. Sequencing was supported by the NASA Astrobiology Institute “From Early Biospheric Metabolisms to the Evolution of complex systems” and performed at the Josephine Bay Paul Center for Comparative Molecular Biology and Evolution at the Marine Biological Laboratory, Woods Hole,

MA. M.A.L. was supported by a Schlanger Ocean Drilling Fellowship, a University of North Carolina Dissertation Completion Fellowship, a Marie-Curie Intra-European Fellowship (number 255135), and funding provided to Bo Barker Jørgensen by the Danish National Research Foundation and Max Planck Society.

The Hanse Wissenschaftskolleg provided a supportive writing environment to A.P.T. during the complex genesis of the manuscript.

We declare that we have no conflicts of interests.

REFERENCES

- Bazylinski DA, Wirsén CO, Jannasch HW. 1989. Microbial utilization of naturally occurring hydrocarbons at the Guaymas Basin hydrothermal vent site. *Appl Environ Microbiol* 55:2832–2836.
- Nelson DC, Wirsén CO, Jannasch HW. 1989. Characterization of large, autotrophic *Beggiatoa* spp. abundant at hydrothermal vents of the Guaymas Basin. *Appl Environ Microbiol* 55:2909–2917.
- Elsgaard L, Isaksen MF, Jørgensen BB, Alayse A-M, Jannasch HW. 1994. Microbial sulfate reduction in deep-sea sediments at the Guaymas Basin hydrothermal vent area: influence of temperature and substrates. *Appl Environ Microbiol* 58:3335–3343.
- Teske A, Hinrichs K-U, Edgcomb V, Gomez AD, Kysela D, Sylva SP, Sogin ML, Jannasch HW. 2002. Microbial diversity of hydrothermal sediments in the Guaymas Basin: evidence for anaerobic methanotrophic

- communities. *Appl Environ Microbiol* 68:1994–2007. <http://dx.doi.org/10.1128/AEM.68.4.1994-2007.2002>.
5. Curray JR, Moore DG, Smith SM, Chase TE. 1982. Underway geophysical data from Deep Sea Drilling Project Leg 64: navigation, bathymetry, magnetics, and seismic profiles, p 505–507. In Blakeslee J, Platt LW, Stout LN (ed), Deep Sea Drilling Initial Reports, vol 64. U.S. Government Printing Office, Washington, DC.
 6. Simoneit BRT, Bode GW. 1982. Carbon/carbonate and nitrogen analyses, Leg 64, Gulf of California, p 1303–1307. In Blakeslee J, Platt LW, Stout LN (ed), Deep Sea Drilling Initial Reports, vol 64. U.S. Government Printing Office, Washington, DC.
 7. Bazylinski DA, Farrington JW, Jannasch HW. 1988. Hydrocarbons in surface sediments from a Guaymas Basin hydrothermal vent site. *Org Geochem* 12:547–559. [http://dx.doi.org/10.1016/0146-6380\(88\)90146-5](http://dx.doi.org/10.1016/0146-6380(88)90146-5).
 8. Martens CS. 1990. Generation of short chain organic acid anions in hydrothermally altered sediments of the Guaymas Basin, Gulf of California. *Appl Geochem* 5:71–76. [http://dx.doi.org/10.1016/0883-2927\(90\)90037-6](http://dx.doi.org/10.1016/0883-2927(90)90037-6).
 9. Pearson A, Seewald JS, Eglington TI. 2005. Bacterial incorporation of relict carbon in the hydrothermal environment of Guaymas Basin. *Geochim Cosmochim Acta* 69:5477–5486. <http://dx.doi.org/10.1016/j.gca.2005.07.007>.
 10. Dhillon A, Lever M, Lloyd KG, Albert DB, Sogin ML, Teske A. 2005. Methanogen diversity evidenced by molecular characterization of methyl coenzyme M reductase A (*mcrA*) genes in hydrothermal sediments of the Guaymas Basin. *Appl Environ Microbiol* 71:4592–4601. <http://dx.doi.org/10.1128/AEM.71.8.4592-4601.2005>.
 11. Holler T, Widdel F, Knittel K, Amann R, Kellermann MY, Hinrichs K-U, Teske A, Boetius A, Wegener G. 2011. Thermophilic anaerobic oxidation of methane by marine microbial consortia. *ISME J* 5:1946–1956. <http://dx.doi.org/10.1038/ismej.2011.77>.
 12. Biddle JF, Cardman Z, Mendlovitz H, Albert DB, Lloyd KG, Boetius A, Teske A. 2012. Anaerobic oxidation of methane at different temperature regimes in Guaymas Basin hydrothermal sediments. *ISME J* 6:1018–1031. <http://dx.doi.org/10.1038/ismej.2011.164>.
 13. Springer E, Sachs MS, Woese CR, Boone DR. 1995. Partial gene sequences for the α subunit of methyl-coenzyme M reductase (*mcrI*) as a phylogenetic tool for the family *Methanosaerinaeae*. *Int J Syst Bacteriol* 45:554–559. <http://dx.doi.org/10.1099/0020713-45-3-554>.
 14. Hallam SJ, Girguis PR, Preston CM, Richardson PM, DeLong EF. 2003. Identification of methyl coenzyme M reductase A (*mcrA*) genes associated with methane-oxidizing Archaea. *Appl Environ Microbiol* 69:5483–5549. <http://dx.doi.org/10.1128/AEM.69.9.5483-5491.2003>.
 15. Lever MA. 2008. Anaerobic carbon cycling pathways in the subseafloor investigated via functional genes, chemical gradients, stable carbon isotopes, and thermodynamic calculations. Ph.D. thesis. University of North Carolina at Chapel Hill, Chapel Hill, NC.
 16. Hales BA, Edwards C, Ritchie DA, Hall G, Pickup RW, Saunders JR. 1996. Isolation and identification of methanogen-specific DNA from blanket bog peat by PCR amplification and sequence analysis. *Appl Environ Microbiol* 62:668–675.
 17. Lever MA, Rouxel OJ, Alt J, Shimizu N, Ono S, Coggon RM, Shans WC III, Lapham L, Elvert M, Prieto-Mollar X, Hinrichs K-U, Inagaki F, Teske A. 2013. Evidence for microbial carbon and sulfur cycling in deeply buried ridge flank basalt. *Science* 339:1305–1308. <http://dx.doi.org/10.1126/science.1229240>.
 18. Ludwig W, Strunk O, Westram R, Richter L, Meier H, Yadhukumar Bucher A, Lai T, Steppi S, Jobb G, Förster W, Brettske I, Gerber S, Ginhart AW, Gross O, Grumann S, Hermann S, Jost R, König A, Liss T, Lüssmann R, May M, Nonhoff B, Reichel B, Strehlow R, Stamatakis A, Stuckmann N, Vilbig A, Lenke M, Ludwig T, Bode A, Schleifer K-H. 2004. ARB: a software environment for sequence data. *Nucleic Acids Res* 32:1363–1371. <http://dx.doi.org/10.1093/nar/gkh293>.
 19. Jones WJ, Leigh JA, Mayer F, Woese CR, Wolfe RS. 1983. *Methanococcus jannaschii* sp. nov., an extremely thermophilic methanogen from a submarine hydrothermal vent. *Arch Microbiol* 136:254–261. <http://dx.doi.org/10.1007/BF00425213>.
 20. Kurr M, Huber R, König H, Jannasch HW, Fricke H, Trincone Kristjansson JK, Stetter KO. 1991. *Methanopyrus kandleri*, gen. and sp. nov. represents a novel group of hyperthermophilic methanogens, growing at 110°C. *Arch Microbiol* 156:239–247. <http://dx.doi.org/10.1007/BF00262992>.
 21. Zhilina TN. 1983. New obligate halophilic methane-producing bacteria. *Microbiology (Engl Transl)* 52:290–297.
 22. Dang H, Luan X, Zhao J, Li J. 2009. Diverse and novel nifH and nifH-like gene sequences in the deep-sea methane seep sediments of the Okhotsk Sea. *Appl Environ Microbiol* 75:2238–2245. <http://dx.doi.org/10.1128/AEM.02556-08>.
 23. Lazar CS, L'Haridon S, Pignet P, Toffin L. 2011. Archaeal populations in hypersaline sediments underlying orange microbial mats in the Napoli Mud Volcano. *Appl Environ Microbiol* 77:3120–3131. <http://dx.doi.org/10.1128/AEM.01296-10>.
 24. Nunoura T, Oida H, Nakaseama M, Kosaka A, Ohkubo SB, Kikuchi T, Kazama H, Hosoi-Tanabe S, Nakamura K, Kinoshita M, Hirayama H, Inagaki F, Tsunogai U, Ishibashi J, Takai K. 2010. Archaeal diversity and distribution along thermal and geochemical gradients in hydrothermal sediments at the Yonaguni Knoll IV hydrothermal field in the Southern Okinawa Trough. *Appl Environ Microbiol* 76:1198–1211. <http://dx.doi.org/10.1128/AEM.00924-09>.
 25. Gieg LM, Davidova IA, Duncan KE, Suflita JM. 2010. Methanogenesis, sulfate reduction and crude oil biodegradation in hot Alaskan oilfields. *Environ Microbiol* 12:3074–3086. <http://dx.doi.org/10.1111/j.1462-2920.2010.02282.x>.
 26. Ver Eecke HC, Butterfield DA, Huber JA, Lilley MD, Olson EJ, Roe KK, Evans LJ, Merkel AY, Cantin HV, Holden JF. 2012. Hydrogen-limited growth of hyperthermophilic methanogens at deep-sea hydrothermal vents. *Proc Natl Acad Sci U S A* 109:13674–13679. <http://dx.doi.org/10.1073/pnas.1206632109>.
 27. Merkel AY, Huber JA, Chernyh NA, Bonch-Osmolovskaya EA, Lebedinsky AV. 2013. Detection of putatively thermophilic anaerobic methanotrophs in diffuse hydrothermal vent fluids. *Appl Environ Microbiol* 79:915–923. <http://dx.doi.org/10.1128/AEM.03034-12>.
 28. Nettmann E, Bergmann I, Pramschüter S, Mundt K, Plogsties V, Herrmann C, Klocke M. 2010. Polyphasic analyses of methanogenic archaeal communities in agricultural biogas plants. *Appl Environ Microbiol* 76:2540–2548. <http://dx.doi.org/10.1128/AEM.01423-09>.
 29. Lazar CS, Parkes RJ, Cragg BA, L'Haridon S, Toffin L. 2011. Methanogenic diversity and activity in hypersaline sediments of the Napoli mud volcano, Eastern Mediterranean Sea. *Environ Microbiol* 13:2078–2091. <http://dx.doi.org/10.1111/j.1462-2920.2011.02425.x>.
 30. Li D, Midgley DJ, Ross JP, Oytam Y, Abell GCJ, Volk H, Daud WAW, Hendry P. 2012. Microbial biodiversity in a Malaysian oil field and a systematic comparison with oil reservoirs worldwide. *Arch Microbiol* 194: 513–523. <http://dx.doi.org/10.1007/s00203-012-0788-z>.
 31. Nercessian O, Bienvenu N, Moreira D, Prieur D, Jeanthon C. 2005. Diversity of functional genes of methanogens, methanotrophs and sulfate reducers in deep-sea hydrothermal environments. *Environ Microbiol* 7:118–132. <http://dx.doi.org/10.1111/j.1462-2920.2004.00672.x>.
 32. Roussel EG, Konn C, Charlou J-L, Donval J-P, Fouquet Y, Querellou J, Prieur D, Cambon Bonavita M-A. 2011. Comparison of microbial communities associated with three Atlantic ultramafic hydrothermal systems. *FEMS Microbiol Ecol* 77:647–665. <http://dx.doi.org/10.1111/j.1574-6941.2011.01161.x>.
 33. Stackebrandt E, Goebel BM. 1994. Taxonomic note: a place for DNA-DNA reassociation and 16S rRNA sequence analysis in the present species definition in bacteriology. *Int J Syst Bacteriol* 44:846–849. <http://dx.doi.org/10.1099/0020713-44-4-846>.
 34. Stackebrandt E. 2009. Phylogeny based on 16S rRNA/DNA. *Encyclopedia of Life Sciences*. Wiley Online Library, Hoboken, NJ. doi:<http://dx.doi.org/10.1002/9780470015902.a0000462.pub2>.
 35. Ollivier B, Cayol J-L, Patel BKC, Magot M, Fardeau M-L, Garcia J-L. 1997. *Methanoplanus petrolearius* sp. nov., a novel methanogenic bacterium from an oil-producing well. *FEMS Microbiol Lett* 147:51–56. <http://dx.doi.org/10.1111/j.1574-6968.1997.tb10219.x>.
 36. Borrel G, O'Toole PW, Harris HMB, Peyret P, Brugère J-F, Gribaldo S. 2013. Phylogenomic data support a seventh order of methylotrophic methanogens and provide insights into the evolution of methanogenesis. *Genome Biol Evol* 5:1769–1780. <http://dx.doi.org/10.1093/gbe/evt128>.
 37. Romesser JA, Wolfe RS, Mayer F, Spiess E, Walther-Mauruschat AW. 1979. *Methanogenium*, a new genus of marine methanogenic bacteria, and characterization of *Methanogenium cariaci* sp. nov. and *Methanogenium marisnigri* sp. nov. *Arch Microbiol* 121:147–153. <http://dx.doi.org/10.1007/BF00689979>.
 38. Wildgruber G, Thomm M, König H, Ober K, Ricchiuto T, Stetter KO. 1982. *Methanoplanus limicola*, a plate-shaped methanogen representing a novel family, the Methanoplanaceae. *Arch Microbiol* 132:31–36. <http://dx.doi.org/10.1007/BF00690813>.

39. L'Haridon S, Reysenbach A-L, Banta A, Messner P, Schumann P, Stackebrandt E, Jeanthon C. 2003. *Methanocaldococcus indicus* sp. nov., a novel hyperthermophilic methanogen isolated from the Central Indian Ridge. *Int J Syst Evol Microbiol* 53:1931–1935. <http://dx.doi.org/10.1099/ijss.0.02700-0.0>.
40. Mikucki JA, Liu Y, Delwiche M, Colwell FS, Boone DR. 2003. Isolation of a methanogen from deep marine sediments that contain methane hydrates, and description of *Methanoculleus submarinus* sp. nov. *Appl Environ Microbiol* 69:3311–3316. <http://dx.doi.org/10.1128/AEM.69.6.3311-3316.2003>.
41. Kendall MM, Liu Y, Sieprawska-Lupa M, Stetter KO, Whitman WB, Boone DR. 2006. *Methanococcus aeolicus* sp. nov., a mesophilic, methanogenic archaeon from shallow and deep marine sediments. *Int J Syst Evol Microbiol* 56:1525–1529. <http://dx.doi.org/10.1099/ijss.0.64216-0.0>.
42. Cheng L, Qiu T-L, Li X, Wang W-D, Deng Y, Yin X-B, Zhang H. 2008. Isolation and characterization of *Methanoculleus receptaculi* sp. nov. from Shengli oil field, China. *FEMS Microbiol Lett* 285:65–71. <http://dx.doi.org/10.1111/j.1574-6968.2008.01212.x>.
43. Wilharm T, Zhilina TN, Hummel P. 1991. DNA-DNA hybridization of methylotrophic halophilic methanogenic bacteria and transfer of *Methanococcus halophilus* to the genus *Methanohalophilus* as *Methanohalophilus halophilus* comb. nov. *Int J Syst Bacteriol* 41:558–562. <http://dx.doi.org/10.1099/00207713-41-4-558>.
44. Cheng L, Qiu T-L, Yin X-B, Wu X-L, Hu G-Q, Deng Y, Zhang H. 2007. *Methermicoccus shengliensis* gen. nov., sp. nov., a thermophilic, methylotrophic methanogen isolated from oil-production water, and proposal of *Methermicoccaceae* fam. nov. *Int J Syst Evol Microbiol* 57:2964–2969. <http://dx.doi.org/10.1099/ijss.0.65049-0>.
45. Whitman WB, Bowen TL, Boone DR. 2006. The methanogenic bacteria, p 165–207. In *Dworkin M, Falkow S, Rosenberg E, Schleifer K-H, Stackebrandt E (ed), The prokaryotes: an evolving electronic resource for the microbiological community*. Springer, New York, NY.
46. Zhang G, Tian J, Jiang N, Guo X, Wang Y, Dong X. 2008. Methanogen community in Zoige wetland of Tibetan plateau and phenotypic characterization of a dominant uncultured methanogen cluster ZC-I. *Environ Microbiol* 10:1850–1860. <http://dx.doi.org/10.1111/j.1462-2920.2008.01606.x>.
47. Boetius A, Ravenschlag K, Schubert CJ, Rickert D, Widdel F, Gieseke A, Amann R, Jørgensen BB, Witte U, Pfannkuche O. 2000. A marine microbial consortium apparently mediating anaerobic oxidation of methane. *Nature* 407:623–625. <http://dx.doi.org/10.1038/35036572>.
48. Orphan VJ, House CH, Hinrichs K-U, McKeegan KD, DeLong EF. 2002. Multiple archaeal groups mediate methane oxidation in anoxic cold seep sediments. *Proc Natl Acad Sci U S A* 99:7663–7668. <http://dx.doi.org/10.1073/pnas.072210299>.
49. Knittel K, Boetius A. 2009. Anaerobic oxidation of methane: progress with an unknown process. *Annu Rev Microbiol* 63:311–334. <http://dx.doi.org/10.1146/annurev.micro.61.080706.093130>.
50. Milucka J, Ferdelman TG, Polerecky L, Franzke D, Wegener G, Schmid M, Lieberwirth I, Wagner M, Widdel F, Kuypers MMM. 2012. Zero-valent sulphur is a key intermediate in marine methane oxidation. *Nature* 491:541–546. <http://dx.doi.org/10.1038/nature11656>.
51. Kellermann MY, Wegener G, Elvert M, Yoshinaga MY, Lin YS, Holler T, Prieto Mollar X, Knittel K, Hinrichs K-U. 2012. Autotrophy as a predominant mode of carbon fixation in anaerobic methane-oxidizing microbial communities. *Proc Natl Acad Sci U S A* 109:19321–19326. <http://dx.doi.org/10.1073/pnas.1208795109>.
52. Teske A, Edgcomb V, Rivers AR, Thompson JR, de Vera Gomez A, Molyneaux SJ, Wirsén CO. 2009. A molecular and physiological survey of a diverse collection of hydrothermal vent *Thermococcus* and *Pyrococcus* isolates. *Extremophiles* 13:905–915. <http://dx.doi.org/10.1007/s00792-009-0278-7>.
53. Canganello F, Jones WJ, Gambacorta A, Antranikian G. 1998. *Thermococcus guaymasensis* sp. nov. and *Thermococcus aggregans* sp. nov., two novel thermophilic archaea isolated from the Guaymas Basin hydrothermal vent site. *Int J Syst Bacteriol* 48:1181–1185. <http://dx.doi.org/10.1099/00207713-48-4-1181>.
54. Burggraf S, Jannasch HW, Nicolaus B, Stetter KO. 1990. *Archaeoglobus profundus* sp. nov., represents a new species within the sulfate-reducing archaeabacteria. *Syst Appl Microbiol* 13:24–28. [http://dx.doi.org/10.1016/S0723-2020\(11\)80176-1](http://dx.doi.org/10.1016/S0723-2020(11)80176-1).
55. Parkes RJ, Linnane CD, Webster G, Sass H, Weightman AJ, Hornbrook ERC, Horsfield B. 2011. Prokaryotes stimulate mineral H₂ forma-
- tion for the deep biosphere and subsequent thermogenic activity. *Geology* 39:219–222. <http://dx.doi.org/10.1130/G31598.1>.
56. Swan BK, Ehrhardt CJ, Reifel KM, Moreno LI, Valentine DL. 2010. Archaeal and bacterial communities respond differently to environmental gradients in anoxic sediments of a California hypersaline lake, the Salton Sea. *Appl Environ Microbiol* 76:757–768. <http://dx.doi.org/10.1128/AEM.02409-09>.
57. Watts JM, Swan BK, Tiffany MA, Hurlbert SH. 2001. Thermal, mixing, and oxygen regimes of the Salton Sea, California, 1997–1999. *Hydrobiologia* 466:159–176. <http://dx.doi.org/10.1023/A:1014599719989>.
58. Zengler K, Richnow HH, Rosselló-Mora R, Michaelis W, Widdel F. 1999. Methane formation from long-chain alkanes by anaerobic microorganisms. *Nature* 401:266–269. <http://dx.doi.org/10.1038/45777>.
59. Nakagawa S, Takai K, Inagaki F, Chiba H, Ishibashi J, Kataoka S, Hirayama H, Nunoura T, Horikoshi K, Sako Y. 2005. Variability in microbial community and venting chemistry in a sediment-hosted back-arc hydrothermal system: impacts of subseafloor phase-separation. *FEMS Microbiol Ecol* 54:141–155. <http://dx.doi.org/10.1016/j.femsec.2005.03.007>.
60. Ehrhardt CJ, Haymon RM, Lamontagne MG, Holden PA. 2007. Evidence for hydrothermal Archaea within the basaltic flanks of the East Pacific Rise. *Environ Microbiol* 9:900–912. <http://dx.doi.org/10.1111/j.1462-2920.2006.01211.x>.
61. Sánchez O, Garrido L, Forn I, Massana R, Maldonado MI, Mas J. 2011. Molecular characterization of activated sludge from a seawater-processing wastewater treatment plant. *Microb Biotechnol* 4:628–642. <http://dx.doi.org/10.1111/j.1751-7915.2011.00256.x>.
62. Pachiadaki MG, Lykousis V, Stefanou EG, Kormas KA. 2010. Prokaryotic community structure and diversity in the sediments of an active submarine volcano (Kazan mud volcano, East Mediterranean Sea). *FEMS Microbiol Ecol* 72:429–444. <http://dx.doi.org/10.1111/j.1574-6941.2010.00857.x>.
63. Zhao L, Ma T, Gao M, Gao P, Cao M, Zhu X, Li G. 2012. Characterization of microbial diversity and community in water flooding oil reservoirs in China. *World J Microbiol Biotechnol* 28:3039–3052. <http://dx.doi.org/10.1007/s11274-012-1114-2>.
64. Keller M, Braun F-J, Dirmeier R, Hafenbrädl D, Burggraf S, Rachel R, Stetter KO. 1995. *Thermococcus calcariphilus* sp. nov., a new hyperthermophilic archaeum growing on polysulfide at alkaline pH. *Arch Microbiol* 164:390–395. <http://dx.doi.org/10.1007/BF02529736>.
65. Kaster KM, Bonaunet K, Berland H, Kjeilen-Eilertsen G, Brakstad OG. 2009. Characterisation of culture-independent and –dependent microbial communities in a high-temperature offshore chalk petroleum reservoir. *Antonie Van Leeuwenhoek* 96:423–439. <http://dx.doi.org/10.1007/s10482-009-9356-1>.
66. Takai K, Gamo T, Tsunogai U, Nakayama N, Hirayama H, Nealson KH, Horikoshi K. 2004. Geochemical and microbiological evidence for a hydrogen-based, hyperthermophilic subsurface lithoautotrophic microbial ecosystem (HyperSLiME) beneath an active deep-sea hydrothermal field. *Extremophiles* 8:269–282. <http://dx.doi.org/10.1007/s00792-004-0386-3>.
67. Yoshida-Takashima Y, Nunoura T, Kazama H, Noguchi T, Inoue K, Akashi H, Yamanaka T, Toki T, Yamamoto M, Furushima Y, Ueno Y, Yamamoto H, Takai K. 2012. Spatial distribution of viruses associated with planktonic and attached microbial communities in hydrothermal environments. *Appl Environ Microbiol* 78:1311–1320. <http://dx.doi.org/10.1128/AEM.06491-11>.
68. Flores GE, Wagner ID, Liu Y, Reysenbach A-L. 2012. Distribution, abundance, and diversity patterns of the thermoacidophilic “deep-sea hydrothermal vent euryarchaeota 2.” *Frontiers Microbiol* 3:1–17. <http://dx.doi.org/10.3389/fmicb.2012.00047>.
69. Schauer R, Røy H, Augustin N, Gennerich H-H, Peters M, Wenzhoefer F, Amann R, Meyer-Dierks A. 2011. Bacterial sulfur cycling shapes microbial communities in surface sediments of an ultramafic hydrothermal vent field. *Environ Microbiol* 13:2633–2648. <http://dx.doi.org/10.1111/j.1462-2920.2011.02530.x>.
70. Weber A, Jørgensen BB. 2002. Bacterial sulfate reduction in hydrothermal sediments of the Guaymas Basin, Gulf of California, Mexico. *Deep Sea Res I* 49:827–841. [http://dx.doi.org/10.1016/S0967-0637\(01\)00079-6](http://dx.doi.org/10.1016/S0967-0637(01)00079-6).
71. Dridi B, Fardeau M-L, Ollivier B, Raoult D, Drancourt M. 2012. *Methanomassiliicoccus luminyensis* gen. nov., sp. nov., a methanogenic archaeon isolated from human faeces. *Int J Syst Evol Microbiol* 62:1902–1907. <http://dx.doi.org/10.1099/ijss.0.033712-0>.

72. Paul K, Nonoh JO, Mikulski L, Brune A. 2012. "Methanoplasmatales," Thermoplasmatales-related Archaea in termite guts and other environments, are the seventh order of methanogens. *Appl Environ Microbiol* 78:8245–8253. <http://dx.doi.org/10.1128/AEM.02193-12>.
73. Takai K, Horikoshi K. 1999. Genetic diversity of archaea in deep-sea hydrothermal vent environments. *Genetics* 152:1285–1297.
74. Vetriani C, Jannasch HW, MacGregor BJ, Stahl DA, Reysenbach A-L. 1999. Population structure and phylogenetic characterization of marine benthic archaea in deep-sea sediments. *Appl Environ Microbiol* 65:4375–4384.
75. Großkopf R, Stubner S, Liesack W. 1998. Novel euryarchaeotal lineages detected on rice roots and in the anoxic bulk soil of flooded rice microcosms. *Appl Environ Microbiol* 64:4983–4989.
76. Inagaki F, Suzuki M, Takai K, Oida H, Sakamoto T, Aoki K, Nealson KH, Horikoshi K. 2003. Microbial communities associated with geological horizons in coastal subseafloor sediments from the Sea of Okhotsk. *Appl Environ Microbiol* 69:7724–7735. <http://dx.doi.org/10.1128/AEM.69.12.7224-7235.2003>.
77. Kubo K, Lloyd KG, Biddle JF, Amann R, Teske A, Knittel K. 2012. Archaea of the Miscellaneous Crenarchaeotal Group are abundant, diverse and widespread in marine sediments. *ISME J* 6:1949–1965. <http://dx.doi.org/10.1038/ismej.2012.37>.
78. Hoehler TM, Alperin MJ, Albert DB, Martens CS. 1998. Thermodynamic control on hydrogen concentrations in anoxic sediments. *Geochim Cosmochim Acta* 62:1745–1756. [http://dx.doi.org/10.1016/S0016-7037\(98\)00106-9](http://dx.doi.org/10.1016/S0016-7037(98)00106-9).
79. Gundersen JK, Jørgensen BB, Larsen E, Jannasch HW. 1992. Mats of giant sulphur bacteria on deep-sea sediments due to fluctuating hydrothermal flow. *Nature* 360:454–456. <http://dx.doi.org/10.1038/360454a0>.
80. Thauer RK. 2011. Anaerobic oxidation of methane with sulfate: on the reversibility of the reactions that are catalyzed by enzymes also involved in methanogenesis from CO₂. *Curr Opin Microbiol* 14:292–299. <http://dx.doi.org/10.1016/j.mib.2011.03.003>.
81. McKay L. 2014. Microbial ecology of a manmade oil spill in the Gulf of Mexico and a natural hydrothermal oil seep in the Gulf of California. Ph.D. thesis. University of North Carolina at Chapel Hill, Chapel Hill, NC.
82. Zehnder AJB, Ingvorsen K, Marti T. 1982. Microbiology of methane bacteria, p 45–68. In Hughes DE, Stafford DA, Wheatley Bl, Baader W, Lettinga G, Nyns EJ, Verstraete W (ed), *Anaerobic digestion*. Elsevier Biomedical Press, Amsterdam, Netherlands.
83. Wellsbury P, Goodman K, Barth T, Cragg BA, Barnes SP, Parkes RJ. 1997. A deep bacterial biosphere fuelled by low-temperature acetate generation during burial. *Nature* 388:573–576. <http://dx.doi.org/10.1038/41544>.
84. Mochimaru H, Uchiyama H, Yoshioka H, Imachi H, Hoaki T, Tamaki H, Nakamura K, Sekiguchi Y, Kamagata Y. 2007. Methanogen diversity in deep subsurface gas-associated water at the Minami-Kanto gas field in Japan. *Geomicrobiol J* 24:93–100. <http://dx.doi.org/10.1080/01490450701266571>.
85. Pham VD, Hnatow LL, Zhang S, Fallon RD, Jackson SC, Tomb JF, DeLong EF, Keeler SJ. 2009. Characterizing microbial diversity in production water from an Alaskan mesothermic petroleum reservoir with two independent molecular methods. *Environ Microbiol* 11:176–187. <http://dx.doi.org/10.1111/j.1462-2920.2008.01751.x>.
86. Orcutt BN, Joye SB, Kleindienst S, Knittel K, Ramette A, Reitz A, Samarkin V, Treude T, Boetius A. 2010. Impact of natural oil and higher hydrocarbons on microbial diversity, distribution, and activity in Gulf of Mexico cold-seep sediments. *Deep Sea Res II* 57:2008–2012. <http://dx.doi.org/10.1016/j.dsri.2010.05.014>.
87. Rinke C, Schwientek P, Sczyrba A, Ivanova NN, Anderson IJ, Cheng J-F, Darling A, Malfatti S, Swan BK, Gies EA, Dodsworth JA, Hedlund HP, Tsiamis G, Sievert S, Liu W-T, Eisen JA, Hallam SJ, Kyrpides NC, Stepanauskas R, Rubin EM, Hugenholtz P, Woyke T. 2013. Insights into the phylogeny and coding potential of microbial dark matter. *Nature* 499: 431–437. <http://dx.doi.org/10.1038/nature12352>.